# THE ROLE OF INDUCED PHASE TRANSFORMATIONS ON FATIGUE PROCESSES IN AISI 304L

Y. Katz, A. Bussiba and H. Mathias *

The fatigue crack propagation behaviour in 304L stainless steel has been investigated. Special attention has been given to the role of austenite stability on the steady state fatigue crack extension stage, and the influencial effects of induced martensitic phases in the case of a load interaction problem. For this purpose studies were carried out by using two types of 304L stainless steels which differed only in terms of the austenite stability degree. Steady state fatigue crack propagation between the $M_s - M_d$ temperatures and the typical retardation behaviour with and without phase transformations are analyzed and discussed.

## INTRODUCTION

In frame of continuous efforts to improve mechanical properties, significant research has been centered on the role of mechanically induced martensitic phases in metastable materials. Mainly the following types of materials have been treated in the literature. Firstly, initially monolithic materials which consist only of the austenitic $\gamma$ phase. Secondly, microduplex structures which contain a fine dispersion of the $\gamma$ phase, either retained or reverted austenite. Along this line, austenitic stainless steels of the 300 grade series (1), ausformed metastable austenitic steels (2) and maraging steels (3) have been investigated. In these studies particular attention has been given to the influence of the $\gamma$ phase stability on the strength, fracture resistance and the fatigue behaviour.

The present paper describes a more detailed study of fatigue crack extension in 304L stainless steel, with emphasis on cycling between the $M_s - M_d$ temperatures. The current study was mainly aimed to elaborate on the possible influences of the induced martensitic phases on the steady-state crack extension, and on the effects of phase transformations in case of a single overload in tension-tension fatigue.

The 304L, that might be thermally stable even down to 4 K, will transform martensitically (below the $M_d$) with a minor assistance of a mechanical driving force. The typical transformation reaction is of the form $\gamma \rightarrow \varepsilon' \rightarrow \alpha'$, where $\varepsilon'$ is the martensitic hexagonal phase and $\alpha'$ is the body centered martensitic phase.

* Nuclear Research Centre-Negev, Beer-Sheva 84 190, Israel.

Clearly, such transformation will take place in 304L by an applied loading, as well as by an internal stress-strain field. Obviously, this will also occur in case of cycling, as actually happens in metastable austenitic materials.

Generally, very little has been done in exploring the role of transformations on fatigue crack propagation processes in a more extended fashion. The work by Chanani et al (4) in Trip steels, and by Bathias and Pelloux (5) in martensitic and austenitic steels and other works (Antolovich et al (6), Hornbogen (7), all deal with the steady-state fatigue crack propagation.

It appears that information regarding the case of single overload, as a simple element of a load interaction problem, might contribute a lot to the mentioned problem. In fact, such an extended programme was adopted in the present study. This approach introduces the effects of the specific plastic-zone microstructure, possible internal stresses due to the $\gamma$-decomposition and the reflection on fatigue crack extension processes.

## EXPERIMENTAL PROCEDURE

Two 304L stainless steels of following chemical compositions (in wt pct) were selected; Cr-18.6;18.7, Ni-9.5;10.2, Mn-1.2;1.1, Mo-0.23;0.20, C-0.03, Si-0.44, S-0.016, P-0.033, Fe-bal. As noticed, the two materials were within the standard composition range of the 304L grade stainless steel, but turned out to differ mainly in the degree of austenite stability.

Standard mechanical properties were established at 296 K and 77 K, including the critical fracture toughness parameters. Preliminary studies were performed regarding the thermo-mechanical $\gamma$-stability of uniform and notched specimens. X-ray diffraction technique and Mössbauer spectroscopy were utilized in order to gather quantitative information in terms of phase concentration values. X-ray diffraction was performed by using $CuK_\alpha$ radiation with a graphite monochrometer. Mössbauer spectroscopy was conducted by a constant acceleration computerized spectrometer using a 25 mCi $^{57}Co(Pd)$ source. More about the exact procedure of phases determination and plastic zone mapping has been described elsewhere (Mathias et al (8), Katz et al (9,10).

Fatigue tests were carried out by using MTS electro-hydraulic closed loop system with an amplitude controller device. Precracked compact tensile specimens of 12 mm in thickness were tested. The cracklength was measured by direct observation and by an electro-potential technique, accompanied by crack-tip-opening displacement (CTOD) measurements and by acoustic emission (AE) monitoring. Steady state fatigue crack propagation rate ( FCPR) curves da/dN vs. the applied nominal $\Delta K$ were determined at 296 K and 77 K. The cyclic nominal $\Delta K$ were calculated by:

$$\Delta K = \frac{\Delta P Y}{B W^{\frac{1}{2}}} \qquad (1)$$

were;

$$Y = 29.6(a/W)^{\frac{1}{2}} - 185.5(a/W)^{\frac{3}{2}} + 655.7(a/W)^{\frac{5}{2}} - 1017(a/W)^{\frac{7}{2}} + 638.9(a/W)^{\frac{9}{2}}$$

$\Delta P$ is the applied cyclic load and a is the crack length. B and W are the specimen thickness and width respectively.

During the whole experimental programme a fatigue frequency of 10 Hz was maintained with $R \simeq 0$.

Actually, the fatigue programme included the steady state crack extension at ambient and at low temperatures, where the latter represented the case of a fatigue process which is associated with a significant amount of induced martensitic phases. In addition, a clear distinction was made between the case of a monolithic $\gamma$ - PZ, caused by the single overload at 296 K, and the case of a multiphase PZ which contained the $\gamma$, $\varepsilon'$ and $\alpha'$ phases. For the multiphase PZ the overload was performed at 77 K, while the subsequent cycling was carried out at room temperature.

For the study of the load transient effects the retardation behaviour was generally compared by considering always a constant PZ. For monolithic $\gamma$-PZ the retardation due to the single overload, for the range $q = K_{ol}/K_{max}$ between 1.5 - 2.65, was previously determined (10). $K_{ol}$ and $K_{max}$ are the stress intensity factor of the single overload and value of the maximum amplitude respectively.

This information served as important comparative background for analysing unique influences of martensitic transformations which occur during the overload cycle.

Clearly, the yield stress values are temperature dependent, and therefore q was modified in order to maintain the same range of PZ sizes for the monolithic and the multiphase single overload. This procedure was performed for the two 304L materials, namely, the more stable (MS) and the less stable (LS) material, as described later on.

## EXPERIMENTAL RESULTS

The mechanical properties for the tested 304L(MS) and 304(LS) materials are given in Table 1. The relatively reduced $\gamma$-stability in the 304(LS) is well reflected in the low elastic limit at 77 K. Actually, the $\gamma$-stability variations dominated the stress-strain curves at 77 K. This was also confirmed by X-ray diffration results. The methods for the quantitative determination of phase concentrations (8) included double checking by X-ray diffraction and Mössbauer spectroscopy.

TABLE 1 - Mechanical Properties.

| Material | Yield Stress 0.2% Offset MPa | | Ultimate Tensile Stress MPa | | Elongation % | | Reduction of Area % | | Critical Fracture Toughness-Kc MPa.m½ | | Hardness $R_B$ | Grain Size μm |
|---|---|---|---|---|---|---|---|---|---|---|---|---|
| | 296K | 77K | 296K | 77K | 296K | 77K | 296K | 77K | 296K | 77K | | |
| 304L-MS | 260 | 510 | 590 | 1350 | 80 | 52 | 72 | 60 | 84 | 130 | 80 | 80 |
| 304L-LS | 340 | 400 | 640 | 1250 | 67 | 33 | 74 | 55 | 90 | 145 | 80 | 40 |

Figure 1 summerizes the austenite decomposition and its dependency on the plastic deformation for uniform specimens of the 304L(MS) steel. As indicated, plastic deformation at 77 K resulted in $\gamma \rightarrow \varepsilon' \rightarrow \alpha'$ transformation with the typical sigmoidal dependency of $\alpha'$ formation on the extent of the plastic strain. Similar induced phases were observed at the vicinity of the crack tip, but clearly controlled by the environment of the sharp stress-strain gradients at the pastic zone. More about this issue has been addressed in previous studies (9,10).

Figure 2 (a) and (b) shows the macroscopic and the microscopic FCPR dependency on the nominal $\Delta K$ at 296 K and 77 K respectively. Generally, at 77 K the microscopic rate indicated some higher values which are attributed to the contribution of alternative modes at low temperatures. However, for specific $\Delta K$ the FCPR values were always lower at 77 K, where induced martensitic phases accompanied the fatigue crack extension stage.

As shown in Table 1, the fundamental monotonic properties are dependent on the temperature. In order to include the thermal effects, a normalization procedure was followed according to Burck and Weertman (11). Here it was assumed that the FCPR is inversely proportional to the plastic work term and the square of a characteristic stress, approximated by the yield or the ultimate stress. This point is shown in Fig. 3, where $f_n$ is the proposed Burck and Weertman function.

Figure 4 illustrates for the 304L(MS) the values of $a - a_o$ for $(da/dN)_{min}$ as a function of the overload parameter q. $\Delta K_{CA}$ is the constant amplitude of the fatige cycling before and after the applied load. As shown, $a - a_o$ for specific fatigue run amplitude is increasing with q. This behaviour differed completely for multiphase PZ. Figure 5 illustrates the multiphase (PZ) retardation behaviour for the 304L(MS) and 304(LS) after overloading at 77 K, and subsequent fatigue cycling at room temperature. The nominal fatigue run consisted of $\Delta K = 22\ MPam^{\frac{1}{2}}$ and $f = 10$ Hz, with an equal overload PZ in both cases.

Figures 6 and 7 show SEM micrographs and the corresponding acoustic emission (AE) signals. In these Figures the cycling load trace is given beside the AE transducer pre-amplified signal. After overloading at 77 K, retardation was readily observed, not only in terms of drastically reduced FCPR, but also by the CTOD and AE results. The CTOD and AE findings provided broadly consistent results, indicating a significant decrease in CTOD and AE activity after the single overload.

## DISCUSSION

The current experimental results actually emphasize the important effects of the induced martensitic phases in fatigue load interaction problems. In contrast to the minor effects in the steady state FCP, the multiphase PZ in single overload resulted in significant influences. Moreover, the retardation behaviour due to the localized inhomogeneous stress-strain field at the crack tip of the multiphase partially transformed PZ differed completely from the behaviour of the monophase PZ.

In the transformed PZ the minimum FCPR occured at a very small value of $a - a_o$, which dominated the whole retardation crack growth curve profile. In fact, only some residual minima were obtained at $a - a_o$, which corresponded to the conventional retardation profile, namely a deformed monophase PZ. This point is mainly stressed by observing the dependency of $(a - a_o)_{min}$ on q, for equal overload plastic zones (Figure 4).

The comparative study between the two series of 304L indicates the role of the stability degree on the retardation intensity and profile (Fig. 5). Moreover, Table 2 shows that for the 304L(LS) actually a FCP arrest occurred. In fact, only for small values of PZ sizes the 304L(MS) and the 304L(LS) behaved similar.

It appears that the ratio between the transformed zone size and the processed fatigue zone size controls the retardation intensity, or the effective factor of the induced martensitic transformation on the FCPR. Thus, in the case of steady state extension, the behaviour of 304L(MS) and the 304L(LS) at 296 K and 77 K was quite similar. Furthermore, the whole curve of FCPR vs. $\Delta K$ remained a monotonic increasing function, without significant scattering even at the higher values of $\Delta K$. At this stage the problem of the steady-state fatigue is not examined in terms of the possible beneficial aspects due to transformed phases.

The main purpose at this point is to stress the unique role of martensitic transformations in case of load interaction problems. The comparison with the normal retardation due to overload in monophase deformed zone really emphasizes the particular effects of the induced martensitic transformation during fatigue crack growth. Hornbogen (7) has studied the influences of transformation in steady-state fatigue, and proposed that transformation effects are caused by the internal compressive stresses which are activated by the positive volume dilatation. Accordingly it seems that in the steady state fatigue the internal stresses could be offset by other parameters (internal stress stability, the intrinsic resistance of the martensite to fatigue crack growth). Thus, in case of the steady-state only mild effects are expected, as ob-

TABLE 2 - Retardation Parameters for a single Overload and transformed Plastic Zone in 304L(MS) and 304L(LS).

| MATERIAL | PZ-SIZE/$\alpha$ mm | $(a-a_o)_{min}$ mm | $(da/dN)_{min}$ mm/cycle | $N_D \times 10^{-5}$ cycles |
|---|---|---|---|---|
| 304L(LS) | 12.9 | - | - | - |
| | 25.9 | 0.23 | $2\times10^{-5}$ | 0.5 |
| | 36.8 | 0.40 | $7\times10^{-7}$ | 2.2 |
| | 48.2 | 0.17 | $5\times10^{-7}$ | 6.0 |
| | 82.5 | - | - | crack arrest |
| 304L(MS) | 15.7 | - | - | - |
| | 22.8 | 0.1 | $3.2\times10^{-5}$ | 0.6 |
| | 46.4 | 0.05 | $2.5\times10^{-6}$ | 1.5 |

tained in the present investgation. This situation alters in the case of single overload, and can probably be formulated by $\Delta K_{eff}$ that with the occurance of phase transformations deviates strongly from $\Delta K_{nominal}$. Thus;

$$\Delta K_{eff} = \Delta K_{nominal} - \Delta K_{trans} \qquad (2)$$

where $\Delta K_{eff}$ is a strongly depentent function of the crack increment $a - a_o$. $K_{trans}$ incorporates the exact geometry mapping of the microduplex PZ, as well as the volume fraction of the transformed phases.

This dependency on $a-a_o$ was really confirmed in the current study by the CTOD results, by the AE response and the fractographic study. The observed fracture modes, after retardation, indicated the local effects of $\Delta K_{eff}$ mainly by the continuous mode transitions, and by the reappearance of striations during the relaxation stage.

Finally, it seems that much more research activity has to be invested in this area in order to refine the view on the role of induced martensitic transformation during fatigue processes, and particularly in the area of load transient effects.

## REFERENCES


1. Hennessy,D., Steckel,G., and Altstetter,C.,1976,Met. Trans. 7A, 415
2. Antolovich,S.D., 1968, Trans. TMS - AIME, 242, 2371
3. Jin,S.,Huang,D.,and Morris,J.W. Jr.,1976,Met.Trans.,7A, 637
4. Chanani,G.R.,Antolovich,S.D.,and Gerberich,W.W.,1972,Met. Trans.,3, 2621
5. Bathias,C.,and Pelloux,R.M.,1973,Met.Trans.,4,1265
6. Antolovich,S.D.,Saxena,A.,and Chanani,G.R.,1974;Met.Trans., 5, 623
7. Hornbogen,E.,1978,Acta Met.,26,147
8. Mathias,H.,Katz,Y.,and Nadiv,S.,1981,"Metal-Hydrogen Systems", T.N. Veziroglu Ed., Pergamon Press.
9. Katz,Y.,Mathias,H.,and Nadiv,S.,1980,"Fracture and Fatigue", J.C.Radon Ed., Pergamon Press.
10. Katz,Y.,Bussiba,A.,and Mathias,H.,1981,"Materials Experimentation and Design in Fatigue", F.Sherratt and J.B.Sturgeon Eds., IPC Press, Guildford, England.
11. Burck,L.H.,and Weertman,J.,1976,Met.Trans.,7A,257

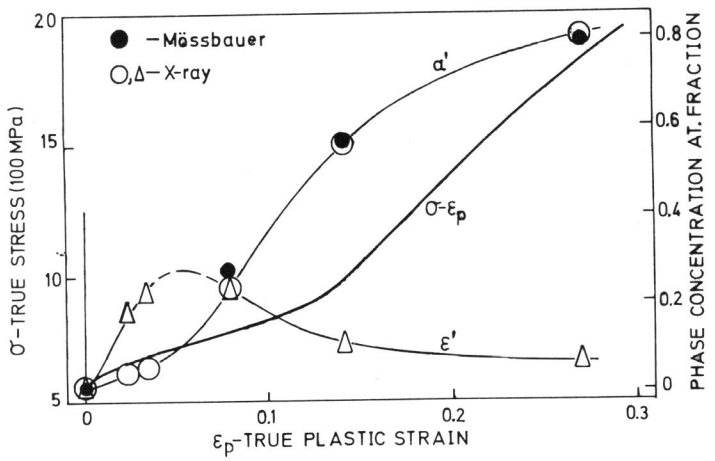


Figure 1 Thermomechanically induced Phases in 304L(MS), strained at 77 K

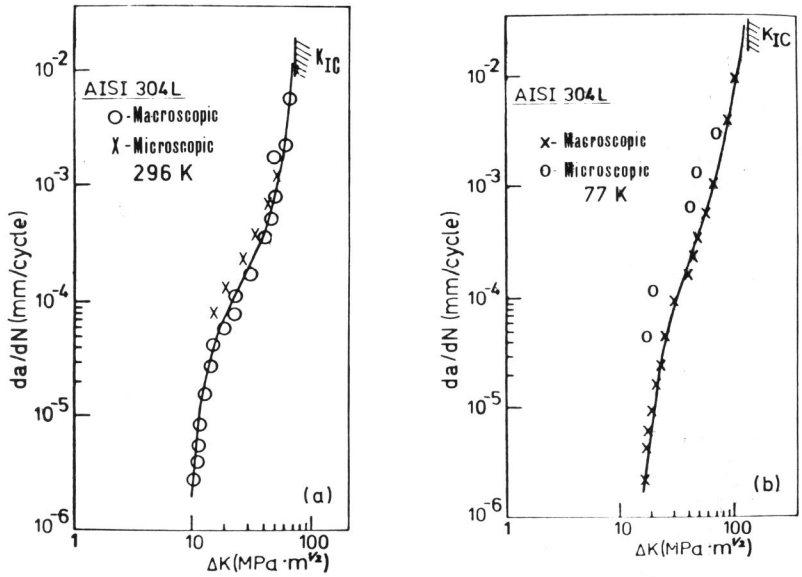


Figure 2 Steady-State FCPR vs. the nominal $\Delta K$. Microscopic rates were based on striation spacings.

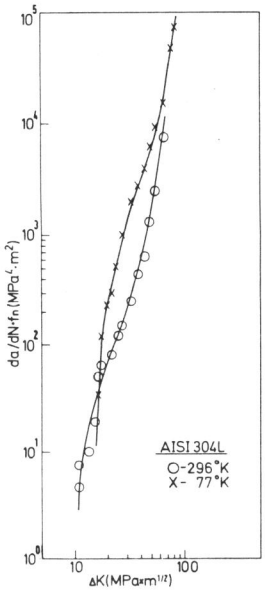


Figure 3 Normalized FCPR curves

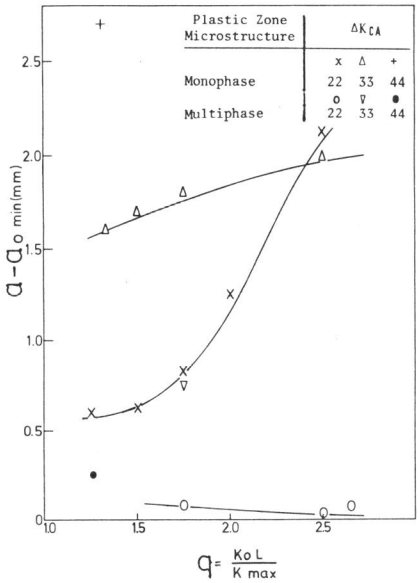


Figure 4 Crack length increments at $(da/dN)_{min}$ vs. q.

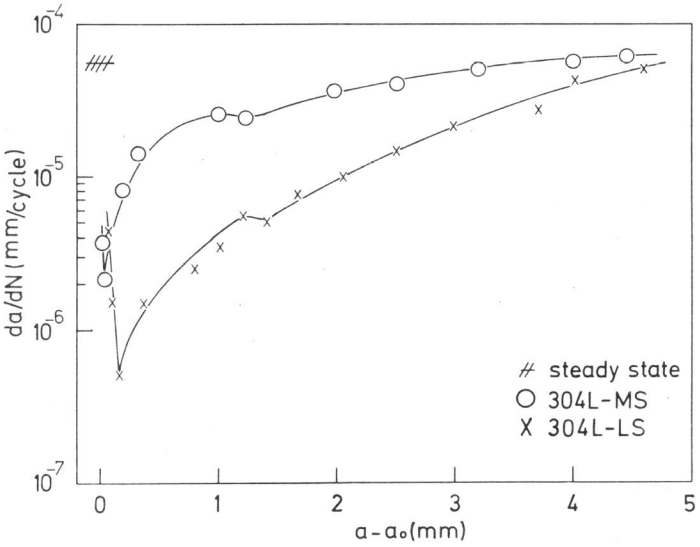


Figure 5 Retardation profiles in overload induced multiphase plastic zones.

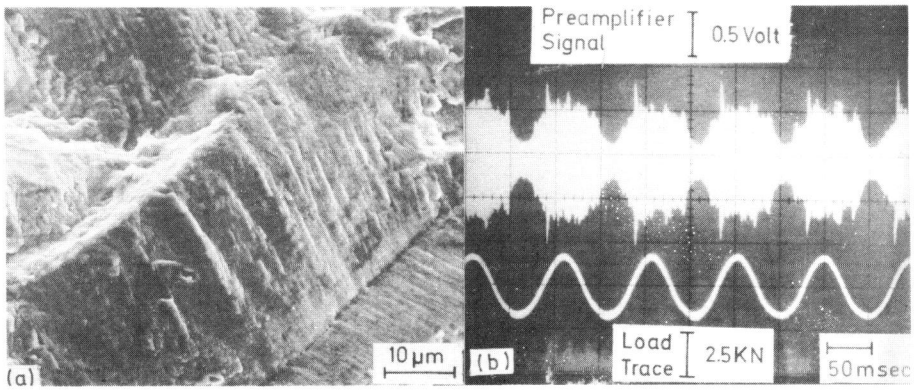


Figure 6 Steady-State Fatigue, (a) SEM micrograph, (b) corresponding acoustic emission signals

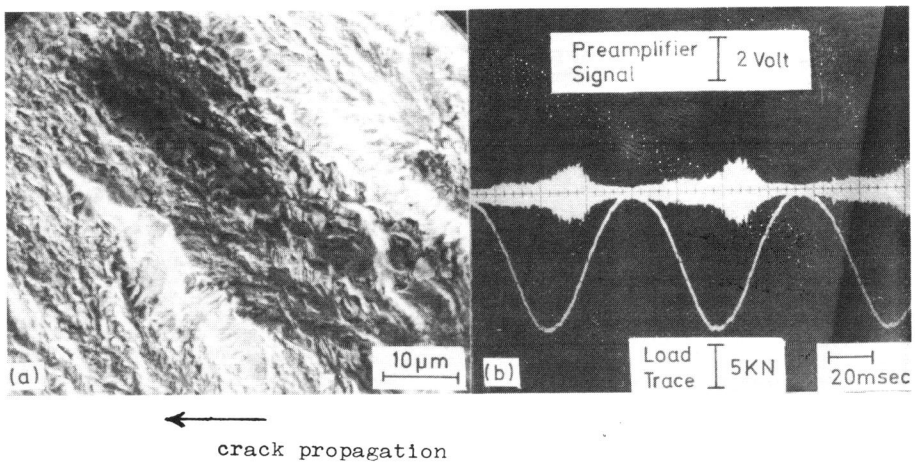


Figure 7 304L(LS) - Multiphase PZ, (a) SEM micrograph, (b) ccrresponding acoustic emission signals